The American Journal of Human Genetics, Volume *93*

Supplemental Data

Mutations in *KLHL40* Are a Frequent

Cause of Severe Autosomal-Recessive

Nemaline Myopathy

Gianina Ravenscroft, Satoko Miyatake, Vilma-Lotta Lehtokari, Emily J. Todd, Pauliina Vornanen, Kyle S. Yau, Yukiko K. Hayashi, Noriko Miyake, Yoshinori Tsurusaki, Hiroshi Doi, Hirotomo Saitsu, Hitoshi Osaka, Sumimasa Yamashita, Takashi Ohya, Yuko Sakamoto, Eriko Koshimizu, Shintaro Imamura, Michiaki Yamashita, Kazuhiro Ogata, Masaaki Shiina, Robert J. Bryson-Richardson, Raquel Vaz, Ozge Ceyhan, Catherine A. Brownstein, Lindsay C. Swanson, Sophie Monnot, Norma B Romero, Helge Amthor, Nina Kresoje, Padma Sivadorai, Cathy Kiraly-Borri, Goknur Haliloglu, Beril Talim, Diclehan Orhan, Gulsev Kale, Adrian K. Charles, Victoria A. Fabian, Mark R. Davis, Martin Lammens, Caroline A. Sewry, Adnan Manzur, Francesco Muntoni, Nigel F. Clarke, Kathryn N. North, Enrico Bertini, Yoram Nevo, Ekkhard Willichowski, Inger E. Silberg, Haluk Topaloglu, Alan H. Beggs, Richard J.N. Allcock, Ichizo Nishino, Carina Wallgren-Pettersson, Naomichi Matsumoto, and Nigel G. Laing

Supplemental Acknowledgments

We would like to thank Naruya Saitou at the National Institute of Genetics for helpful comments on computation of the mutational age. The authors acknowledge the facilities and the scientific and technical assistance of the Australian Microscopy & Microanalysis Research Facility at the Centre for Microscopy, Characterisation, and Analysis at The University of Western Australia, a facility funded by the University, State, and Commonwealth Governments. Thanks to Dr. David Margulies and the Boston Children's Hospital Gene Partnership Program for assistance with whole exome sequencing.

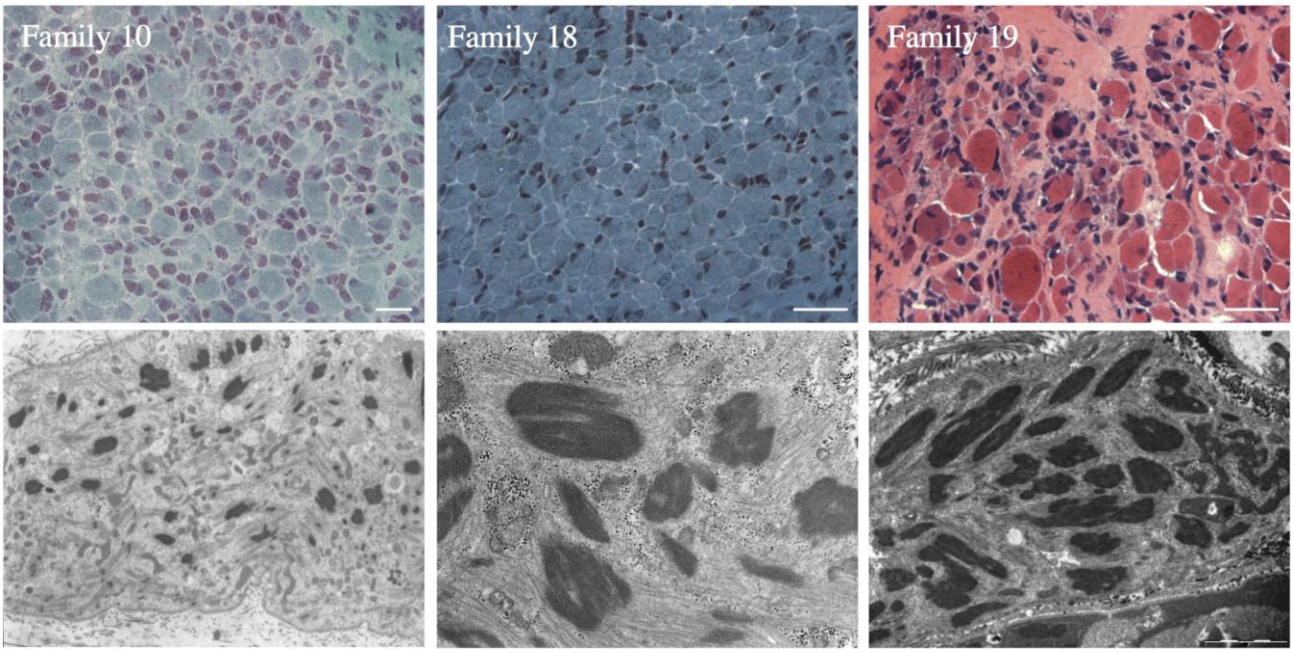

Figure S1. Muscle Microscopy

Gomori trichrome (families 10 [II-1] and 18 [II-2]) and H&E staining (family 19) of affected individuals' muscle biopsies showing abnormal variation of myofiber size with many small myofibers, and increased connective tissue, and the presence of numerous red-stained nemaline bodies (in Gomori trichrome staining), sometimes only visible with high power optics (scale bars: 20 μm). Electron microscopy showed many nemaline bodies, of varying size and shape, in *KLHL40*-NEM biopsies.

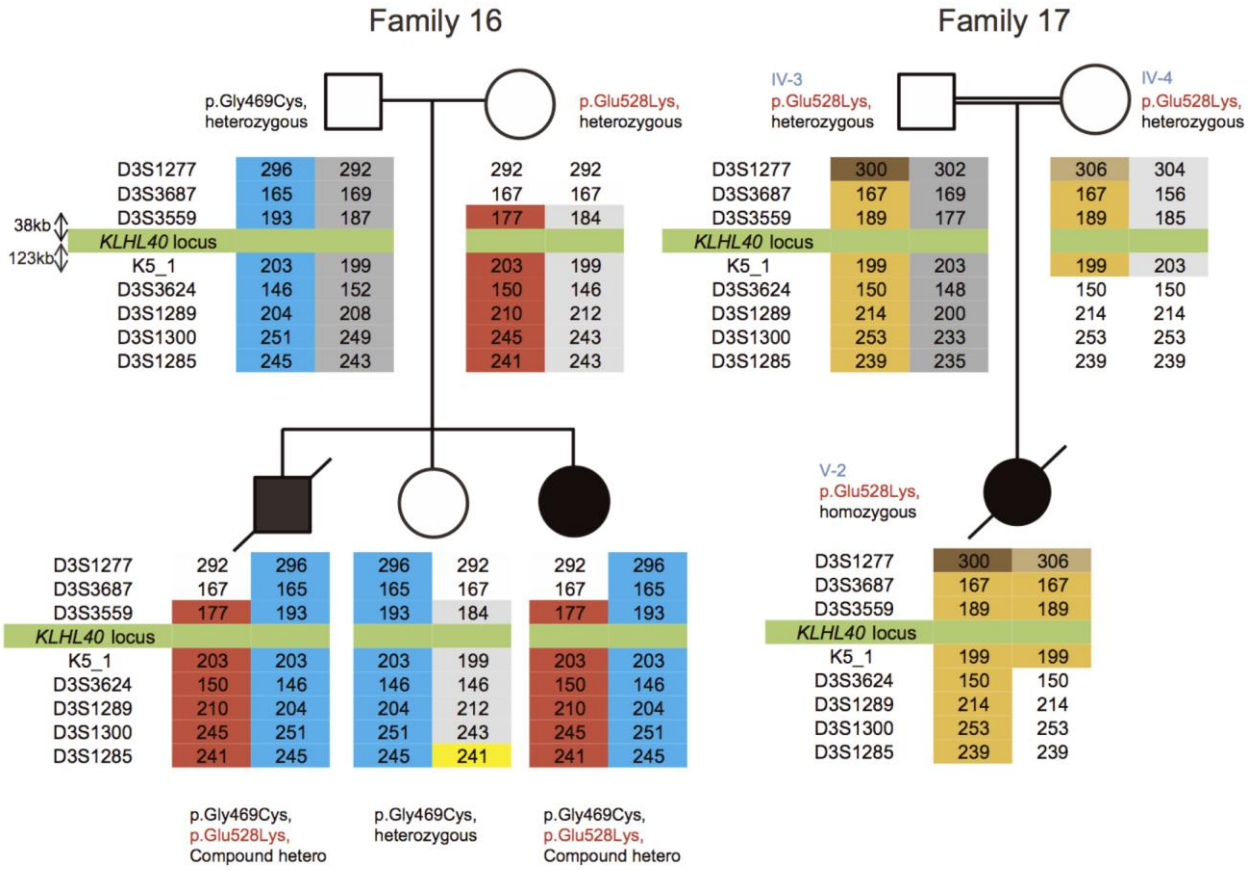

Figure 2. Haplotype Analysis of Families 16 (Japanese) and 17 (Turkish) around the *KLHL40* Locus

STR-markers around the *KLHL40* locus (D3S1277, D3S3687, D3S3559, D3S3624, D3S1289, D3S1300, D3S1285, and the in-house (Yokohama) designed TG repeat marker at 42857630-42857822 on Chr3) were used for haplotype analysis. STRs were amplified with fluorescently-labeled primers and fragment analysis was performed by ABI Genetic Analyzer 3500xL and Genemapper v4.1 (Applied Biosystems). K5_1 represents the originally designed TG repeat marker mapped to 42857630-42857822 on Chr3. D3S3559 is located 38-kb upstream, and K5_1 is located 123-kb downstream of the *KLHL40* locus. Common haplotypes were not recognized among the c.1582G>A variant carriers from the two pedigrees. Blue highlighted block: Japanese-family specific disease haplotype associated with c.1405G>T, red block: Japanese-family specific disease haplotype associated with c.1582G>A, orange block: Turkish-family specific disease haplotype associated with c.1582G>A, yellow block: suspected recombination, and un-highlighted block: uninformative markers.

Figure 3. Clustal Alignment of Human BTB-Kelch Proteins and KLHL40 Sequences for Different Species

Residues that harbor missense substitutions are highlighted in red and the mutated amino acids shown below the alignments.

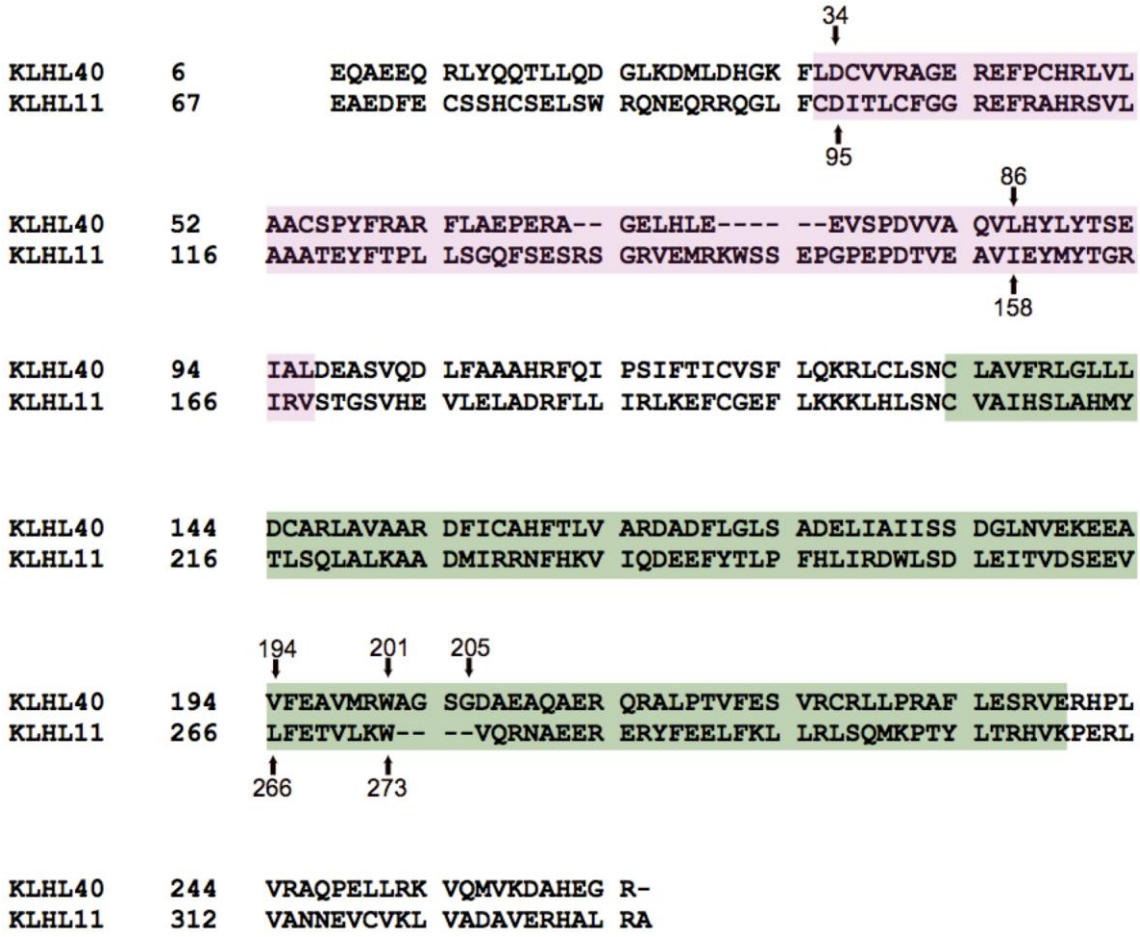

Figure S4. Alignment of the BTB-BACK Domains of KLHL40 and KLHL11

Alignment of the translated amino acid sequence of the BTB-BACK domains of human KLHL40 (UniProtKB Q2TBA0) and KLHL11 (UniProtKB Q9NVR0) using HHPred. Pink and green shading indicates the BTB and the BACK domains, respectively. Arrows indicate the positions of substituted residues.

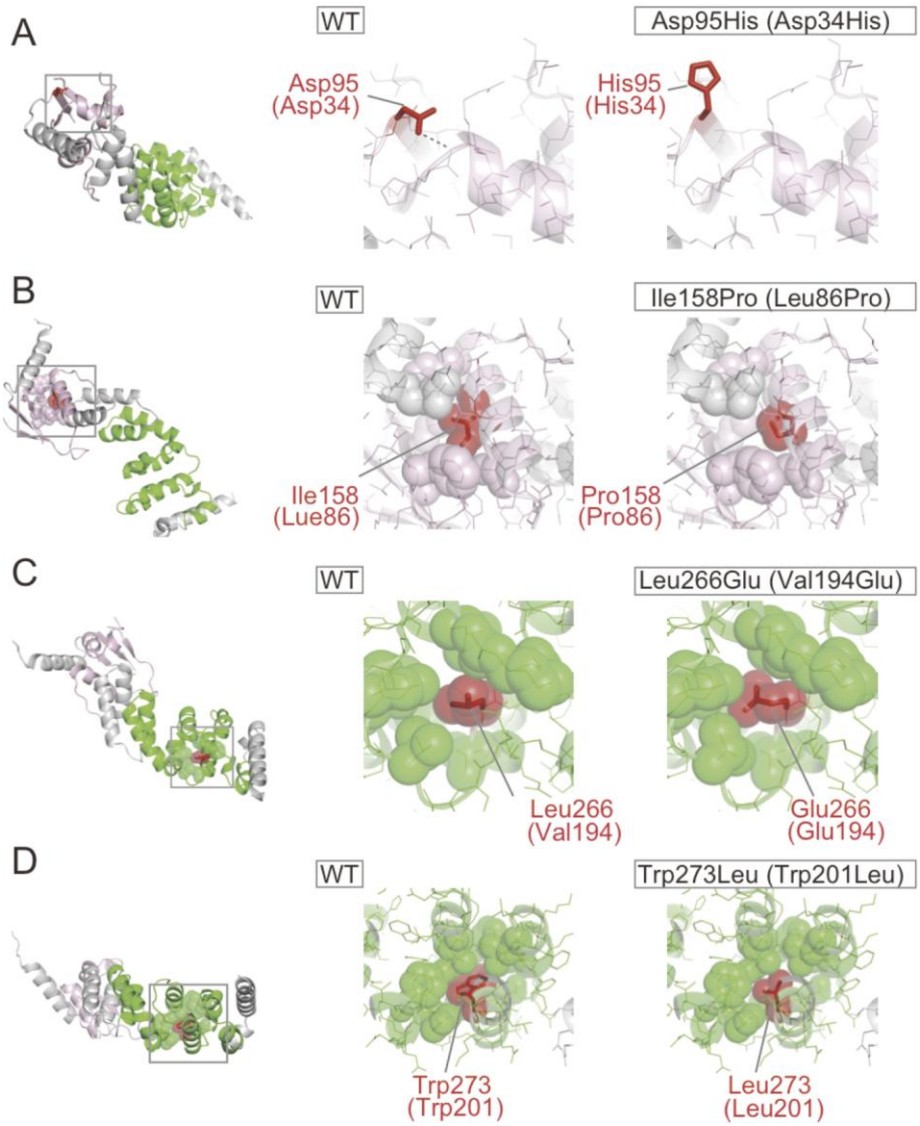

Figure S5. Structural Modeling of the Missense KLHL40 Substitutions on BTB-BACK Domain Structures

Impact of the p.Asp34His (A), p.Leu86Pro (B), p.Val194Lys (C) and p.Trp201Leu (D) substitutions on the BTB-BACK domain structures. Overall (left) and close-up views of the wild-type crystal structure (center) and its modeled mutant structures (right) of the BTB-BACK domain of human KLHL11 (PDB code 3I3N) are shown. Amino acid residues at the positions of 95, 158, 266 and 273 of human KLHL11, which correspond to those of 34, 86, 194 and 201 of human KLHL40, are shown as sticks with van der Waals spheres in red. Side chains of some residues forming the hydrophobic core around the substituted residues are shown in transparent van der Waals representation in (B)–(D). α-helices and loops are drawn as opaque ribbons, arrows and threads in an overall view (left) and as transparent ones in close-up views (center and right). In close-up views, the stick model structure is also shown, and a hydrogen bond is depicted as a gray dotted line. Indicated residue numbers refer to human KLHL11 with those corresponding to human KLHL40 in parentheses. The substitutions were introduced *in silico* using FoldX. Colors are as in Figure 2.

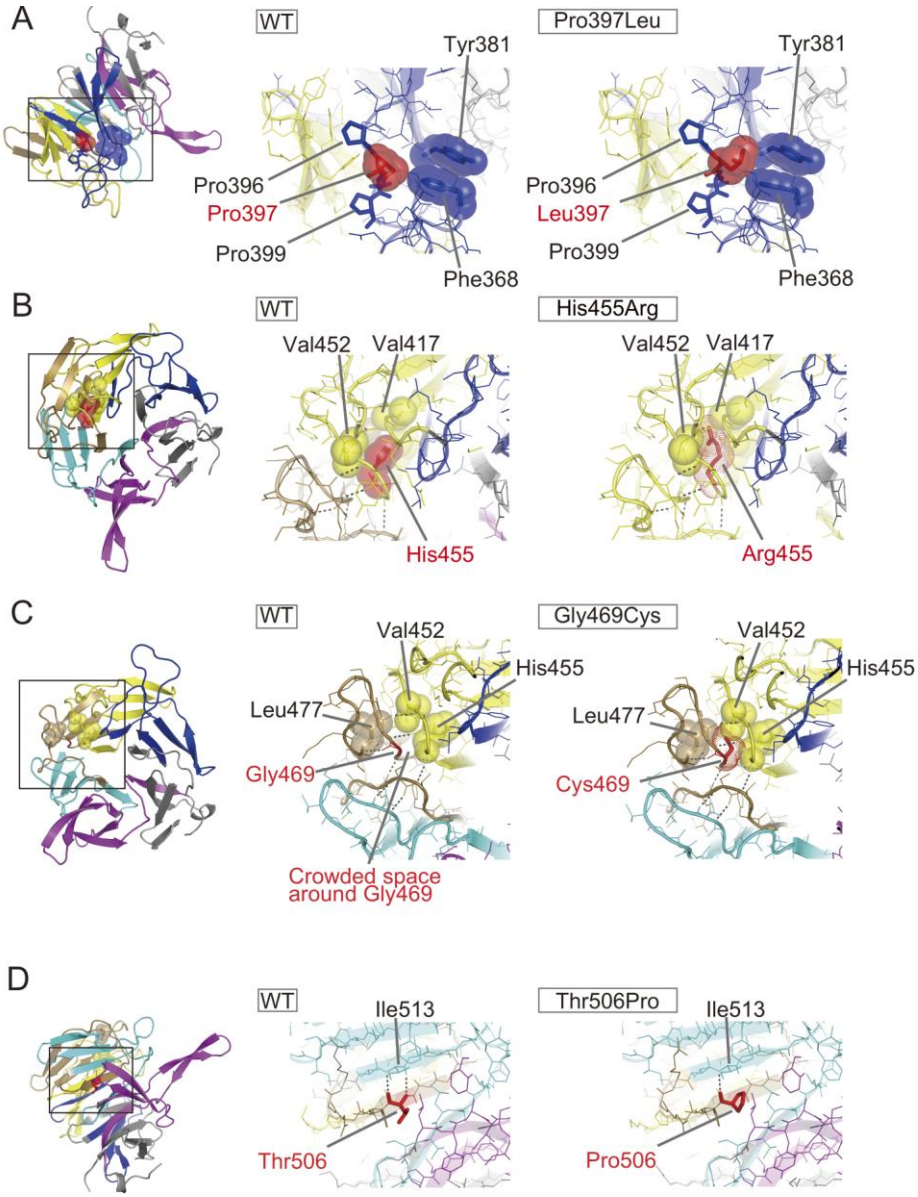

Figure S6. Structural Modeling of the Missense KLHL40 Substitutions on the Kelch Domain Structure

Impact of the p.Pro397Leu (A), p.His455Arg (B), p.Gly469Cys (C) and p.Thr506Pro (D) substitutions on the Kelch domain structure. Overall (left) and close-up views of the wild-type crystal structure (center) and its modeled mutant structures (right) of the Kelch domain of human KLHL40 are shown with indications of amino acid residues involved in interactions with the substituted residues, which are colored in red. The substituted residues and the surrounding residues involved in hydrophobic cores are shown as sticks with van der Waals transparent spheres or, in the case of the mutated Arg455 (B, right) and Cys469 (C, right) residues, van der Waals dots. In (A), the residues which form a type II polyproline helix are shown as sticks. β-sheets and loops are drawn as opaque arrows and threads in an overall view (left) and as transparent ones in close-up views (center and right). The stick model structure is also shown in close-up views. The substitutions were introduced *in silico* using FoldX. Colors are as in Figure 2.

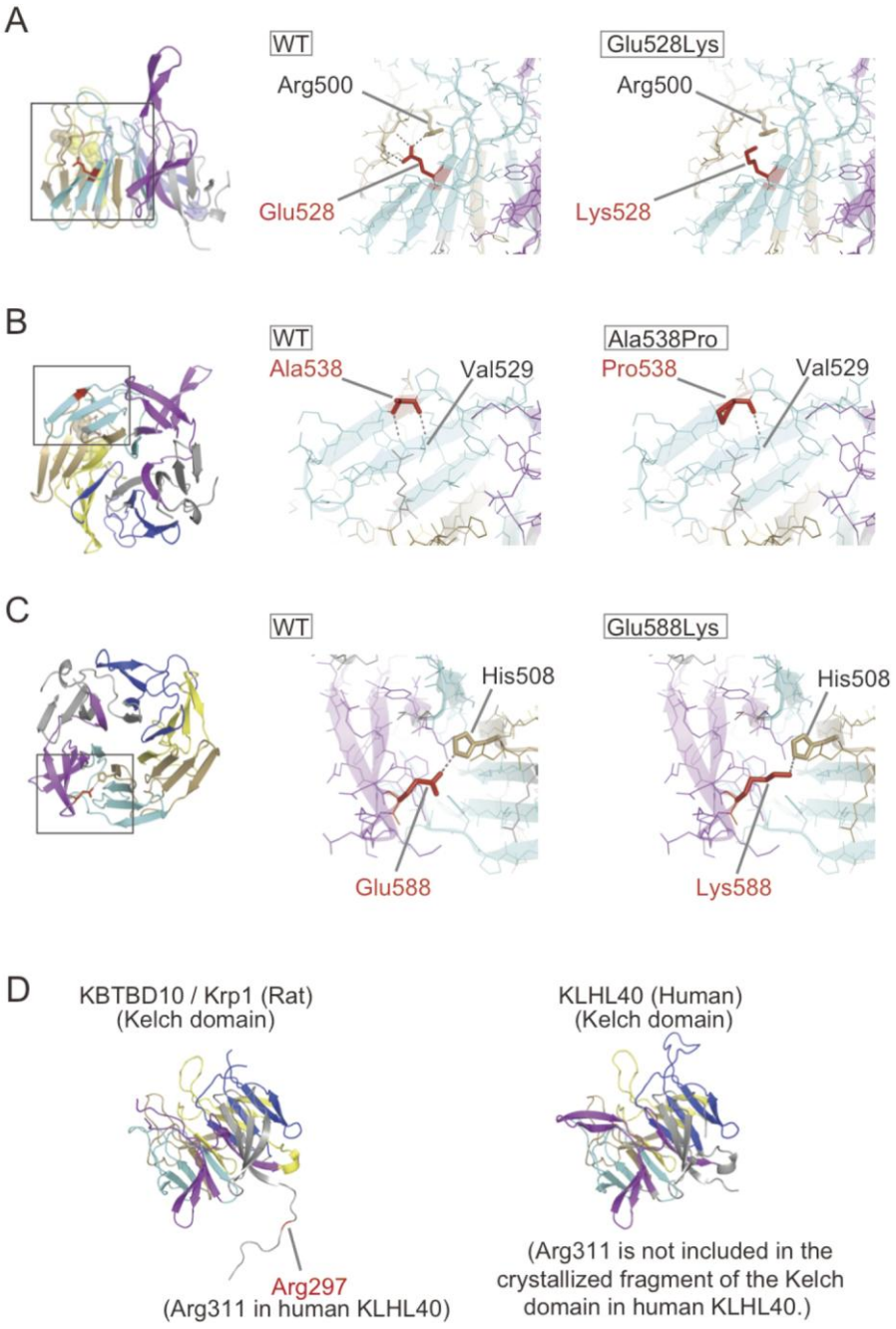

Figure S7. Structural Modeling of the Missense KLHL40 Substitutions on the Kelch Domain Structure (Continued)

(A–C) Impact of the p.Glu528Lys (A) and p.Ala538Pro (B) and p.Glu588Lys (C) substitutions on the Kelch domain structure. The substituted residues and their interacting residues are shown as sticks. β-sheets and loops are drawn as opaque arrows and threads in an overall view (left) and as transparent ones in close-up views (center and right). The stick model structure is also shown in close-up views. Hydrogen bonds are depicted as gray dotted lines. Colors are as in Figure 2.

(D) Location of Arg311 in KLHL40. Crystal structures of the Kelch domains of rat Kelch repeat and BTB (POZ) domain containing 10 (KBTBD10/Krp1; PDB code 2WOZ) and human KLHL40 (PDB code 4ASC) are shown with indication of the position of Arg297 in rat KBTBD10/Krp1 corresponding to Arg311 in human KLHL40.

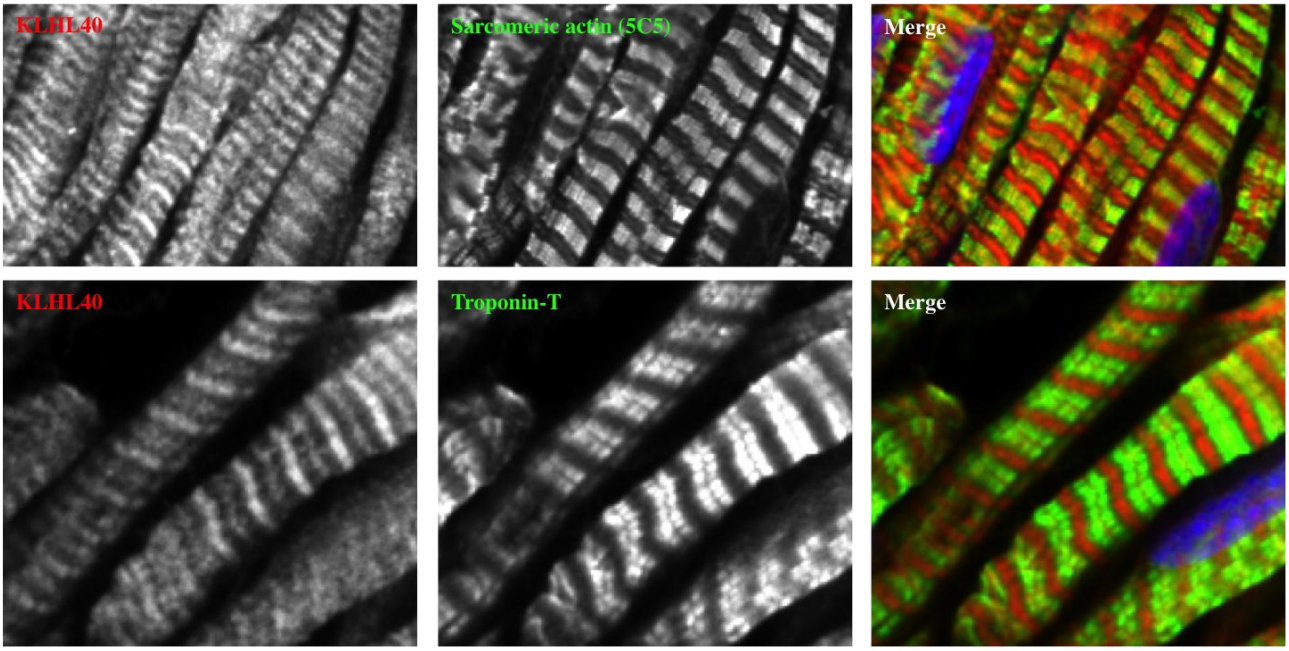

Figure S8. Confocal Microscopy of Fetal Human Skeletal Muscle Costained for KLHL40 and Thin Filament Markers

Sections of human fetal skeletal muscle (31 weeks gestation) were colabeled with the KLHL40 antibody and a monoclonal troponin-T antibody or a monoclonal antibody to sarcomeric α-actin (clone 5C5).

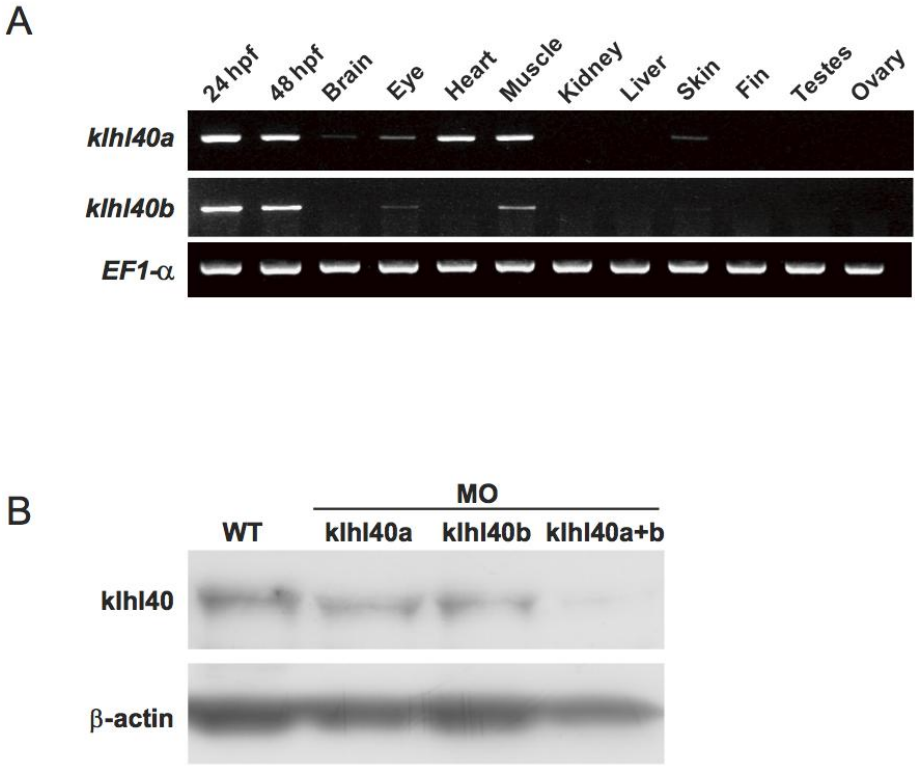

Figure S9. *klhl40* Expression in Zebrafish and Morpholino Knockdown

(A) RT-PCR analysis demonstrating expression of both *klhl40a* and *klhl40b* in the zebrafish at 24 and 48 hours postfertilization (hpf). In adult tissues strong bands are observed for *klhl40a* in the heart and skeletal muscle with faint bands detected in the brain, eye, and fin. Adult expression of *klhl40b* is detected in the muscle, with faint bands in the eye and fin.

(B) Efficacy of the *klhl40a*-MO and *klhl40b*-MO was demonstrated by loss of Klhl40a and Klhl40b and both Klhl40a/40b in immunoblot analysis using an antibody raised against the C-terminal of KLHL40. β-actin was used as a loading control. Dechorionated embryos at 24 hpf were lysed, and immunoblotting was performed using antibodies against KLHL40 (KBTBD5; 1:1,000 dilution, ARP39889_P050; Aviva Systems Biology) and β-actin (1:5,000 dilution, ab6276; Abcam). Positive signals were detected using an ECL kit.

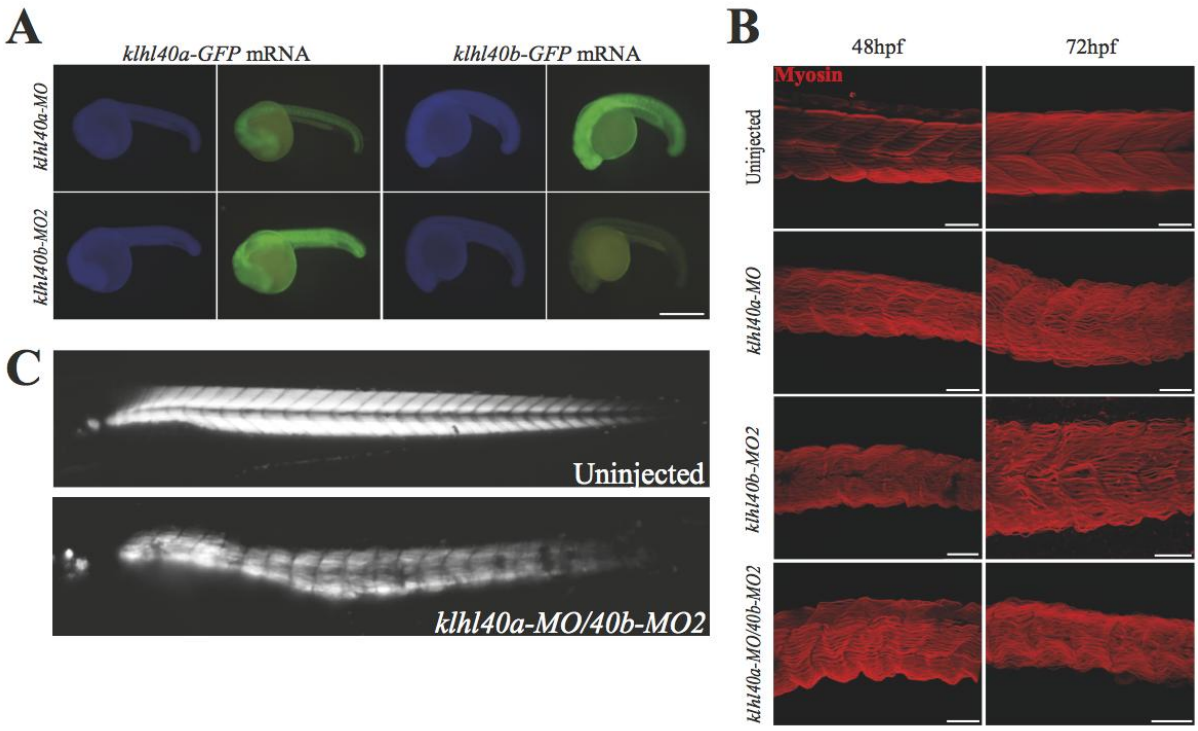

Figure S10. *klhl40* Morpholino Knockdown and Double Knockdown

(A) Green fluorescent protein (GFP) mRNA in which the initiation sequence had been replaced by the *klhl40a*-MO or k*lhl40b*-MO2 target site was injected into embryos. Co-injection of *klhl40a*-MO or *klhl40b*-MO2 demonstrated the inhibition of GFP translation. Injection of *klhl40a*-MO into klhl40b-GFP mRNA injected embryos or injection of *klhl40b*-MO2 into klhl40a-GFP mRNA injected embryos showed no effect. Cascade blue was used as an injection control. Scale bar: 500 µm. Efficacies of *klhl40a*-MO and *klhl40b*-MO2 were tested by co-injecting mRNA containing the MO target sequence fused with eGFP. eGFP reporter constructs were generated (Table S1) and amplified sequences were cloned into pCS2+ vector. mRNA was produced using the mMESSAGE mMACHINE kit (Life Technologies), and injected at 12.5ng/µl.

(B) Knockdown of either Klhl40a or Klhl40b (*klhl40b*-MO2) results in severe disruption of the skeletal muscle with fibers appearing wavy and extensive gaps between fibers in contrast to the densely packed and aligned fibers of the uninjected controls. Embryos injected with both morpholinos show only a slight increase in severity. Maximum intensity projection images from confocal image series following immunolabeling with an antibody to myosin (clone A4.1025).

(C) *klhl40a*-MO/*40b*-MO2 double morphant fish at 72 hpf display a greatly altered birefringence pattern compared to uninjected controls, indicating wide-spread disruption of the sarcomeric register. Scale bar: 50 µm.

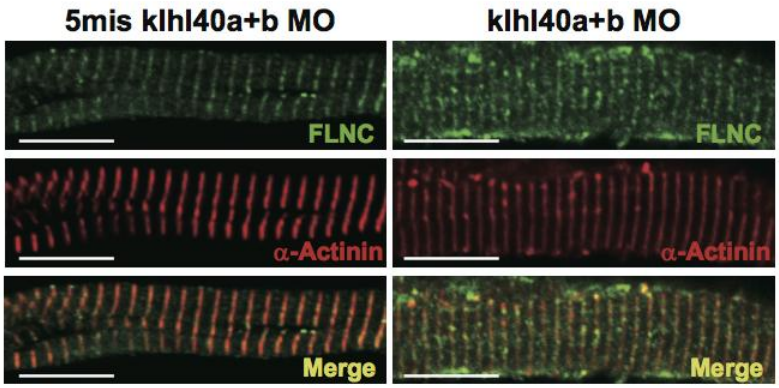

Figure S11. Isolation of Myofibers from *klhl40a*-MO/*40b*-MO Double Morphants Showed an Aggregation of Z-Disk Proteins, Suggesting the Presence of Nemaline Bodies

Confocal micrographs following immunolabeling with an antibody to FLNC (HPA006135) and α-actinin in isolated myofibers from 5mis injected and *klhl40a*-MO/*40b*-MO injected embryos. Scale bar: 10 μm.

Table S1. Primer and Morpholino Sequences for Zebrafish Studies

Primer Sequences for Amplification of Zebrafish *klhl40a* and *klhl40b* cDNA	
klhl40a forward primer:	5'-ATGGCCTCCATGTCAGTGGA-3'
klhl40a reverse primer	5'-ATTCCATGGCCATAAACTGC-3'
klhl40b forward primer	5'-CATCAGGCTACGTCTGGTTCCTCGG-3'
klhl40b reverse primer	5'-CTCCATGGCCATACACTAGGTAGG-3'
Primer Sequences for RT-PCR of Zebrafish *klhl40a* and *klhl40b*	
klhl40a forward primer	5′-CCACAAAGGATTGGTCTACGTGA-3′
klhl40a reverse primer	5′-CGCCAACATTGTCATTAATGTGTAAGG-3′
klhl40b forward primer	5′-TAGTGTATGGCCATGGAGTTGTG-3′
klhl40b reverse primer	5′-AGATTTTGGTGCAGTGAATGATTGG-3′
Sequences for Antisense Morpholinos Zebrafish *klhl40a* and *klhl40b*	
klhl40a-MO	5′-GGTCCACTGACATGGAGGCCATCTT-3′
klhl40b-MO	5′-AGAGCCATGCTGACTGTCTTCAATC-3′
klhl40b-MO2	5′-GGTAGAGCCATGCTGACTGTCTTCA-3′
Primers for eGFP Reporter Constructs	
klhl40a forward primer	5'-AAGATGGCCTCCATGTCAGTGGACCTTGTGAGCAAGGGCGAGGAGCTGTTCAC-3’
klhl40b forward primer	5'-TGAAGACAGTCAGCATGGCTCTACCTGTGAGCAAGGGCGAGGAGCTGTTCAC-3'
reverse primer (*klhl40a* and *klhl40b*)	5'-TTACTTGTACAGCTCGTCCATGCCG-3'

Table S2. Heterozygous *KLHL40* Variants of Uncertain Significance

Family	Variant	PolyPhen 2.0	SIFT	Mutation Taster	Provean	Incidence EVS; 1000 Genomes
Family 1	c.50C>G (p.Thr17Arg)	Probably Damaging (0.997)	Tolerated (0.33)	Disease Causing (0.999)	Damaging (-2.606)	ND; ND
Family 35	c.361G>A (p.Val121Met)	Possibly Damaging (0.617)	Damaging (0.01)	Disease Causing (0.999)	Tolerated (-1.235)	ND; ND
Family 36	c.362T>C (p.Val121Ala)	Benign (0.003)	Tolerated (0.13)	Disease Causing (0.999)	Tolerated (-0.804)	ND; ND
Family 4	c.521_523delCCG (p.Ala174del)	NA	NA	Polymorphism (0.883)	Damaging (-8.760)	NA; ND
Family 33	c.956T>C (p.Leu319Pro)	Probably Damaging (1.000)	Damaging (0)	Disease Causing (0.999)	Damaging (-2.816)	ND; ND

This table shows the single heterozygous variants identified in five additional NEM families. The interpretation of these variants by various mutation prediction programs are shown as are the incidences of these variants within the NHLBI Exome Sequencing Project database (EVS) and the 1000genomes browser. NA: not available; ND: not detected.

Table S3. Detailed Clinical Features of NEM Cases Found to Have *KLHL40* Mutations

Family	Cases	Nationality	Sex (M/F)	Age (age at death)	Family history	Prenatal period		Neonatal period			Facial involvement		Dysphagia	Muscle weakness	Contractures at birth	Fractures at birth	Others
						Prenatal symptoms	Fetal akinesia/ hypokinesia	Birth age	BW	Asphyxia/ respiratory failure	Facial weakness	Minor dysmorphology					
F2	Helsinki No.120	Italian	M	(2mo)	+	+	+	36w	2735g	++	++	NI	++	+++	+	+	
F3	BOS1191	Turkish	M	6mo	+	+	+	34w	2500g	++	++	NI	++	+++	+	+	Chest deformity, Microgenitalia, Intellectual disability, Heart defect
F5	Helsinki No. 253	Israeli	M	(2yrs)	+++	+	+	41w	3020g	+	+	NI	++	++	+	-	Chest deformity, Hypertension
			M	(1.5 yrs)		+	+	32w	1200g	+	+	NI	++	++	NI	-	Chest deformity, Hyperthyroidism
F6	II-2; Helsinki No. 18	Turkish	M	8yrs	+++	NI	NI	NI	NI	NI	NI	NI	NI	NI	NI	NI	
F7	Helsinki No. 3793	Norwegian	M	(9d)	-	+	+	36w	1775 g	++	+	+	++	+++	+	-	
F9	Helsinki No. 161	Turkish	M	(3d)	+++	+	NI	37w	2130g	+	NI	NI	NI	+++	+	NI	Chest deformity
F10	II-1	Chinese	M	(5d)	-	+	+	36w	NI	++	+	+	+	+++	-	-	Chest deformity, Finger and/or foot deformities
F12	J11	Japanese	M	3yrs	-	+	+	34w	2122g	+	+	NI	+	++	+	+	Chest deformity, Brain abnormality
F13	J10	Korean	F	6mo	-	+	NI	36w	2646g	+	+	+	+	+	+	NI	Brain abnormality
F14	Helsinki No. 5423	Turkish	M	(4 mo)	+++	-	-	41w	3330g	++	+	NI	++	+++	+	-	Finger and/or foot deformities
F15	J12	Japanese	M	3mo	-	+	NI	37w	2412g	+	++	+	+	++	+	+	Chest deformity, Microgenitalia
F16	II-3	Japanese	F	1yr	+	+	+	38w	2660g	+	+	+	++	++	+	+	Anemia
	II-1		M	(1yr)		+	NI	38w	2500g	+	+	+	++	++	+	-	
F17	V-2	Turkish	F	(3.5mo)	+++	+	+	34w	2590g	++	+	+	++	+++	+	+	Chest deformity, Finger and/or foot deformities, Cardiac insufficiency, Heart defect, Pulmonary hypertension
	V-3		F	(20d)		+	+	37w	2580g	++	+	+	++	+++	+	+	Chest deformity, Finger and/or foot deformities
F18	II-2	Kurdish	M	(10mo)	+++	+	+	39w	3380g	+	+	+	++	+++	+	-	Chest deformity, Finger and/or foot deformities
F19	Helsinki No. 195	Kurdish	M	11yrs	+	-	-			++	+	+	++	+	-	-	Chest deformity, Finger and/or foot deformities, Spine deformity, Improved markedly, walks with an aid.
F20	J1	Japanese	F	1.5yrs	NI	NI	NI	NI	NI	NI	NI	NI	NI	NI	NI	NI	
F21	J2	Japanese	F	3mo	NI	NI	NI	NI	NI	NI	NI	NI	NI	NI	NI	NI	
F22	J3	Japanese	F	1mo	-	-	-	37w	2400g	+	+	NI	+	++	NI	NI	
F23	J4	Japanese	F	1mo	NI	+	NI	40w	2846g	+	+	+	+	++	+	NI	
F24	J5	Japanese	M	3mo	+	+	NI	41w	2410g	+	++	NI	+	+	+	NI	Chest deformity
F25	J6	Japanese	F	6mo	-	-	-	39w	2505g	+	+	NI	+	++	+	+	Chest deformity
F26	J7	Japanese	M	8mo	-	+	NI	38w	2640g	+	NI	+	+	+	+	NI	Finger and/or foot deformities, Microgenitalia, Spine deformity
F27	J8	Japanese	F	10mo	NI	+	+	38w	3300g	+	NI	NI	NI	+	+	NI	Finger and/or foot deformities
F28	J9	Japanese	M	11mo	-	-	-	42w	2660g	+	+	NI	+	++	+	NI	Chest deformity, Spine deformity
F29	Helsinki No. 388	Turkish	M	(15d)	++	+	+	34w	2030g	++	+	NI	NI	+++	+	+	Finger and/or foot deformities
F30	Helsinki No. 66 (5663)	Turkish	F	(1hr)	+++	+	NI	40w	NI	+	NI	+	++	+++	+	NI	Pulmonary hypoplasia
F31	II-2; BOS74	Vietnamese	F	(30d)	+	+	+	38w	2429g	++	++	NI	NI	+++	+	+	Chest deformity, Brain abnormality
	II-4; BOS74		M	NI	+	+	+	35w	2515g	++	NI	+	NI	+++	+	NI	Microgenitalia
F34	Helsinki No. 254	Turkish	F	20yrs	-	+	+	NI	3200g	-	NI	NI	-	+	-	-	Ambulant, Non-progressive, Motor milestones not delayed.

Family History; +: positive affected sibs or spontaneous abortions, ++: positive consanguinity, +++: both positive affected sibs and consanguinity. Asphyxia/Respiratory Failure; +: present, ++: ventilator required. Facial Weakness; +: present, ++: with ophthalmoparesis. Dysphagia; +: present, ++: tube-feeding/gastrostomy required. Muscle Weakness; +: present, ++: severe, +++: no movement. NI: no information; -: not present.